BIOCHEMISTRY
including biophysical chemistry & molecular biology

Article

pubs.acs.org/biochemistry

Unfolding Action of Alcohols on a Highly Negatively Charged State of Cytochrome *c*

Pulikallu Sashi, U. Mahammad Yasin, and Abani K. Bhuyan*

School of Chemistry, University of Hyderabad, Hyderabad 500 046, India

Supporting Information

ABSTRACT: It is well-known that hydrophobic effect play a major role in alcohol−protein interactions leading to structure unfolding. Studies with extremely alkaline cytochrome *c* (U_B state, pH 13) in the presence of the first four alkyl alcohols suggests that the hydrophobic effect persistently overrides even though the protein carries a net charge of −17 under these conditions. Equilibrium unfolding of the U_B state is accompanied by an unusual expansion of the chain involving an intermediate, I_{alc}, from which water is preferentially excluded, the extent of water exclusion being greater with the hydrocarbon content of the alcohol. The mobility and environmental averaging of side chains in the I_{alc} state are generally constrained relative to those in the U_B state. A few nuclear magnetic resonance-detected tertiary interactions are also found in the I_{alc} state. The fact that the I_{alc} state populates at low concentrations of methanol and ethanol and the fact that the extent of chain expansion in this state approaches that of the U_B state indicate a definite influence of electrostatic repulsion severed by the low dielectric of the water/alcohol mixture. Interestingly, the $U_B \rightleftharpoons I_{alc}$ segment of the $U_B \rightleftharpoons I_{alc} \rightleftharpoons U$ equilibrium, where U is the unfolded state, accounts for roughly 85% of the total number of water molecules preferentially excluded in unfolding. Stopped-flow refolding results report on a submillisecond hydrophobic collapse during which almost the entire buried surface area associated with the U_B state is recovered, suggesting the overwhelming influence of hydrophobic interaction over electrostatic repulsions.

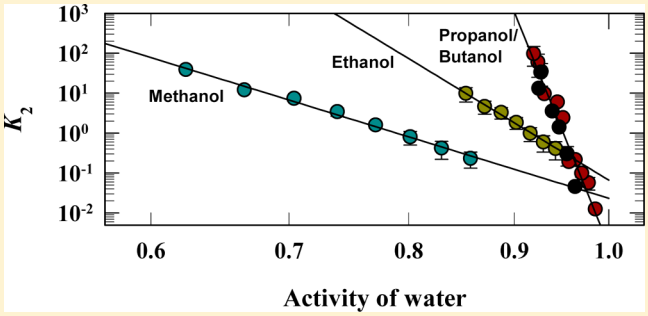

It has been 50 years since studies of the effect of alcohol on protein stability began.[1−4] Analyses of alcohol-induced protein unfolding data augmented by theories of Peller,[5] Flory,[6] and Nemethy and Scheraga[7] soon suggested that alcohols predominantly act by disrupting the hydrophobic interactions in proteins, consistent with the observation that the effectiveness of unfolding varies commensurate with the size of the hydrocarbon functional of alcohols.[4,8] It was also observed that alcohols somehow induced helix formation concomitant with disruption of the tertiary fold,[5,9−13] a finding that attracted the attention of numerous subsequent studies.[14−29] These investigations appeared to suggest that alcohols exert an effect on local hydrogen bonding interactions such as those in secondary structures indirectly by influencing the properties of the bulk solvent, and that the electrostatic mechanism has little role to play. Most recent work considers the importance of both hydrophobic interaction and hydrogen bonding[30] and, from a thermodynamic viewpoint, suggests that alcohols provide a much wider range of temperatures in which the protein stays stable.[31]

Although hydrophobic interaction has been unambiguously implicated, the significance and the mechanism of alcohol-mediated secondary structure promotion remain unclear. The relative importance of not only hydrophobic interaction and hydrogen bonding but also the physical properties of the water/alcohol binary solvent that influence temporal and equilibrium phenomena of the protein is not certain. Further, to what extent can the importance of electrostatic interaction be dismissed? Testing the role of protein charges in alcohol-induced unfolding requires conditions under which the net charge on the protein is greatly enhanced so that electrostatic interactions can no longer be ignored. On the basis of this rationale, we initiated a study of alcohol-induced unfolding of cytochrome *c* under extreme alkaline conditions (pH 13) where the protein is highly negatively charged with stronger electrostatic repulsions because of the exclusion of ionic strength. A drastic reduction of the electrostatic free energy can disrupt the electrostatic balance of protein charges. Such conditions also discourage hydrogen-bonded local interactions because the solution pH fairly approaches the pK_a values of peptide amide hydrogens. Results can then be analyzed to extract information about hydrodynamic properties, populations of intermediates, and temporal hydrophobic collapse.

The choice of extreme alkaline cytochrome *c*, called the U_B state, for these experiments was driven by available information about the thermodynamic and electrostatic properties, and the folding−unfolding behavior of the protein under these conditions,[32−36] even though the heme protein is probably not the best system for studying protein−alcohol interaction presumably because of direct binding of methanol to the Fe^{3+} of cytochrome *c*.[37] However, alcohols are known to bind to

Received: November 16, 2011
Revised: March 2, 2012
Published: March 22, 2012

protein apolar sites in general, and in many cases, the OH group also establishes hydrogen bonding interactions with polar residues.[38,39] The U_B state transforms to an orthodox molten globule (B state) when Na^+ ions are added,[33] and the experiments of this study are conducted simply by replacing NaCl with linear alcohols. Because the dielectric constant is an inverse function of the electrostatic free energy, a large increase in the electrostatic free energy in the presence of alcohols can be highly destabilizing. At equilibrium, alcohol unfolding of the U_B state is described by a $U_B \rightleftharpoons I_{alc} \rightleftharpoons U$ model, where I_{alc} is an intermediate, but temporally, a burst hydrophobic collapse produces an intermediate that appears to be topologically similar to the U_B state. Preferential solvation, tertiary contacts, and the hydrodynamic radius of the equilibrium intermediate have been determined by fluorescence and nuclear magnetic resonance (NMR) methods. The results suggest the overwhelming influence of hydrophobic collapse over electrostatic interaction.

MATERIALS AND METHODS

Alcohol Titration of Alkaline Cytochrome *c*. Two stock solutions of precisely 10 μM protein and pH 13 were prepared, one in water (native stock) and the other in 60−80% of the alcohol (unfolded stock). Different volumes of the two stock solutions were mixed to obtain 0.5 mL of samples that differed only in the mole fraction of the alcohol. This procedure of sample preparation also aims to establish the reversibility of the folding−unfolding reaction. Samples were incubated for 5−6 h at 23 ± 1 °C before fluorescence emission spectra were recorded in the 300−400 nm region via excitation at 280 nm. The sample pH read after measurement was invariably 13.

Stopped-Flow Kinetics. For refolding, an ∼200 μM cyt *c* solution was prepared in 45−60% alcohol (pH 13). Following incubation for 2 h at 23 ± 1 °C, refolding was initiated by 8-fold stopped-flow dilution of the protein solution into water/alcohol mixtures (pH 13) with different alcohol contents. The same procedure was applied to unfolding experiments for which the initial protein solution (∼200 μM) was prepared in water at pH 13. After kinetics had been recorded, the waste solutions were collected to check the pH. A Biologic SFM-400 mixing module with a 0.8 mm cuvette (FC 08) thermostated at 23 ± 0.5 °C was used to record fluorescence-probed kinetics. The excitation wavelength was 280 nm, and emission was measured using a 320 nm cutoff filter. Typically, 10−12 shots were averaged. The measured dead time was 1.3 ± 0.2 ms.

NMR Spectroscopy. Cytochrome *c* solutions (1 μM) were prepared in CD_3OD/D_2O solutions (pH 13). Phase sensitive NOESY spectra (τ_m = 150 ms) were recorded with 512 t_1 points and a 8012 Hz spectral width. Paramagnetically shifted resonances are not excited in this spectral width. Pulsed-field-gradient NMR (PFG NMR) diffusion measurements were taken with a diffusion gradient (*z*-gradient) strength in the range of 3−50 G cm^{-1}. These spectra were of 32K complex data points for a spectral width of 8012 Hz. Approximately 0.5 mM 1,4-dioxane was included in the protein samples for the internal R_h standard. Values of R_h were calculated by

$$I(g) = A \exp(-kg^2)$$

$$R_h^{protein} = R_h^{dioxane}\left(\frac{k_{dioxane}}{k_{protein}}\right) \quad (1)$$

where *I* and *g* are the NMR signal intensity and gradient strength, respectively. The decay constant, *k*, is proportional to the diffusion coefficient. NMR spectra were recorded at 23 ± 1 °C in a 500 MHz Avance III spectrometer (Bruker).

RESULTS

Qualitative Description of Unfolding of Alkaline Cyt *c* in Water/Alcohol Cosolvents. Nativelike states of cyt *c* are fluorescence-silent because of the transfer of excitation energy between the indole of the lone tryptophan (W59) and the heme group. An increase in the spatial proximity of the two groups caused by polypeptide chain expansion renders W59 fluorescent, which is the hallmark of global structural unfolding of cyt *c*. Figure 1

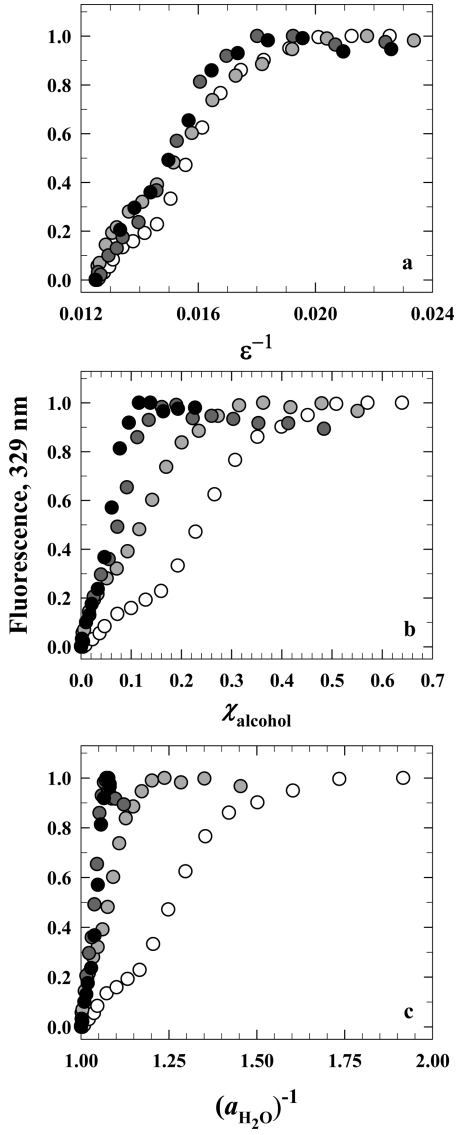

Figure 1. Alcohol-induced unfolding of the U_B state of cyt *c*. (a) The chain expansion seems to be dependent only on the dielectric constant of the solvent containing methanol (○), ethanol (light gray circles), propanol (dark gray circles), or butanol (●). (b) Effectiveness of the alcohols clearly seen in the mole fraction scale. Symbols for alcohols are the same as in panel a. A three-state transition ($U_B \rightleftharpoons I_{alc} \rightleftharpoons U$, where the intermediate I_{alc} accumulates) is clearly seen for methanol (○) and ethanol (light gray circles), although the $U_B \rightleftharpoons I_{alc}$ and $I_{alc} \rightleftharpoons U$ transitions are not clearly resolved because of the strong unfolding effect of propanol (dark gray circles) and butanol (●). (c) Unfolding transition as a function of water activity that allows determination of preferential hydration. Symbols are the same as in panels a and b.

dx.doi.org/10.1021/bi201716r | *Biochemistry* 2012, 51, 3273−3283

shows this effect due to the action of the aliphatic alcohols, methanol, ethanol, propanol, and butanol. The data contain information about both the mechanism of unfolding action of alcohol and a thermodynamically stable structural intermediate involved in chain expansion. With regard to the effect of solution properties, the unfolding equilibrium seems fairly invariant to the alcohol type when the static dielectric constant of the water/alcohol binary solvent alone is considered (Figure 1a), appearing to suggest that it is the macroscopic dielectric property of the solvent that drives the equilibrium. However, because a specific value of the bulk dielectric constant is obtained for different mole fractions of alcohols, their molar volumes should also be considered. On this basis, Figure 1b distinguishes the unfolding equilibria according to mole fractions of different alcohols, suggesting that the surface area of the alcohol that directly influences the physical property of the binary solvent system cannot be ignored. Even more relevant are the decreasing mole fraction of water and alcohol-induced changes in the water activity coefficient, leading to a departure of its activity ($a_w = m_w\gamma_w$, where m_w and γ_w are the mole fraction and activity coefficient of water, respectively) from ideality. The relevance is contained in the fact that the activity dependence of the unfolding equilibrium constant quantifies changes in solvation during protein unfolding.[40] The plot of fluorescence versus $a_{H_2O}^{-1}$ also distinguishes the unfolding transition according to the structural bulkiness of alcohols (Figure 1c). With regard to the structural mechanism of unfolding, primary inspection of the data indicates a three-state equilibrium unfolding transition

$$U_B \overset{K_1}{\rightleftharpoons} I_{alc} \overset{K_2}{\rightleftharpoons} U$$

where U_B and U are compact denatured and expanded unfolded states, respectively, and I_{alc} is an intermediate characterized by a partly expanded polypeptide. The intermediate populates under conditions where the activity of water has not sufficiently deviated from ideality (Figure 1c).

Preferential Exclusion of Water and Interaction with Alcohol during Protein Unfolding. Quantification of preferential interaction of solvents with cyt *c* requires evaluation of the two equilibrium constants, K_1 and K_2, corresponding to the $U_B \rightleftharpoons I_{alc} \rightleftharpoons U$ mechanism, as a function of cosolvent activity according to Wyman, Tanford, Timashesff, and others.[40−42] One may choose to analyze the functional dependence of K_i on water activity because it is the preferential interaction with water that seems to determine the functional properties of proteins. The analysis is based on the following[42,43]

$$\frac{\partial \ln K}{\partial \ln a_{H_2O}} = \Delta\zeta_w = \left(\frac{\partial m_w}{\partial m_p}\right)^{U}_{T,P,\mu_w} - \left(\frac{\partial m_w}{\partial m_p}\right)^{N}_{T,P,\mu_w} \quad (2)$$

where $\Delta\zeta_w$ is the difference between the preferential binding of water to the native and unfolded states, m_w and m_p represent molal concentration of water and protein, respectively, and μ_w is the chemical potential of water. Data in Figure 1c allow for calculation of values of both K_1 and K_2 for methanol and ethanol, but only a single equilibrium constant ($K \sim K_2$), the values of which are very similar for propanol and butanol and could be obtained due to indistinguishable $U_B \rightleftharpoons I_{alc}$ and $I_{alc} \rightleftharpoons U$ transitions. In fact, the instability of I_{alc} in the presence of these two alcohols causes the species not to accumulate. For both methanol and ethanol, the $(\partial \ln K_1)/(\partial \ln a_w)$ gradient corresponding to the conversion of the native state to the intermediate, $U_B \rightleftharpoons I_{alc}$, is significantly sharper than the $(\partial \ln K_2)/(\partial \ln a_w)$ gradient that represents the unfolding transition of the intermediate, $I_{alc} \rightleftharpoons U$ (Figure 2a), and the

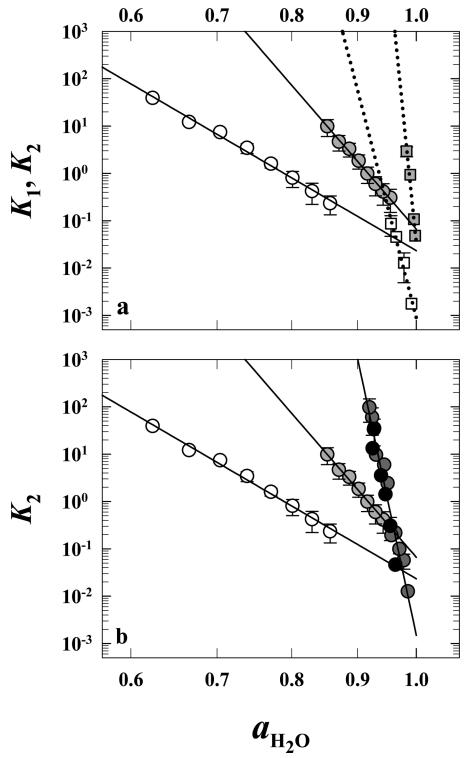

Figure 2. Plots of the logarithm of equilibrium constants K_1 (I_{alc}/U_B) and K_2 (U/I_{alc}) according to the $U_B \rightleftharpoons I_{alc} \rightleftharpoons U$ mechanism as a function of water activity. (a) The K_1 slope for both methanol (□) and ethanol (gray squares) is significantly steeper than the corresponding K_2 slope (white and gray circles), suggesting that the $U_B \rightleftharpoons I_{alc}$ step accounts for most of the water molecules preferentially excluded from the protein during the unfolding reaction. The total number of excluded water molecules is the sum of the numbers for the two steps (Table 1). (b) The K_2 slopes for methanol (○), ethanol (light gray circles), propanol (dark gray circles), and butanol (●) suggest that the number of excluded water molecules grows with the increasing hydrophobicity of the alkyl chain of the alcohol (Table 1).

variation of the $(\partial \ln K_2)/(\partial \ln a_w)$ gradient with the type of alcohol is depicted in Figure 2b. Values of $\Delta\zeta_w$ extracted from slopes of these Wyman plots are listed in Table 1.

The magnitude of $\Delta\zeta_w$ could be interpreted to reflect the change in the effective number of water molecules that interact with the protein during unfolding.[43] Thus, the formation of the intermediate I is accompanied by net departure of 105 water molecules ($\Delta\zeta_w = -105$) when the process is induced by methanol, but a net of 268 water molecules depart ($\Delta\zeta_w = -268$) during ethanol-induced unfolding (Table 1). However, there are significantly fewer net water molecules exchanged during the $I_{alc} \rightleftharpoons U$ transition: 22, 36, and 137 for methanol, ethanol, and propanol or butanol, respectively. Three important results emerge. First, the changes in protein hydration and water exchange events in the unfolding of alkaline cyt *c* are largely completed in the first stage of the reaction in which the native protein transforms to an intermediate ($U_B \rightleftharpoons I_{alc}$), suggesting the similarity of the I_{alc} and U forms in terms of water hydration. Second, the bulkiness of the hydrocarbon functional of the alcohol that determines the acid−base properties of its OH functional considerably influences polypeptide hydration changes across the unfolding transition: the bulkier the hydrophobic hydrocarbon group, the larger the change

dx.doi.org/10.1021/bi201716r | *Biochemistry* 2012, 51, 3273−3283

Table 1. Numbers of Water Molecules ($\Delta\zeta_w$) Preferentially Excluded from the Protein Domain in the Three-State Unfolding ($N \rightleftharpoons I_{alc} \rightleftharpoons U$) of Alkaline Cytochrome *c*[a]

		$\Delta\zeta_w$	
reaction	alcohol	pH 13	pH 7[b]
$U_B \rightleftharpoons I_{alc}$	methanol	−105 ± 8	
	ethanol	−268 ± 9	
$I_{alc} \rightleftharpoons U$	methanol	−22 ± 6	
	ethanol	−36 ± 5	
$U_B \rightleftharpoons U$	propanol/butanol	−137 ± 10[c]	
$N \rightleftharpoons U$	methanol		−20 ± 5
	ethanol		−35 ± 7
	propanol		−160 ± 10

[a]The negative sign with $\Delta\zeta_w$ values indicates the departure of water with unfolding. [b]The unfolding reaction is an apparently two-state reaction ($N \rightleftharpoons U$). [c]The error shown may be underestimated because of the very poor resolution of the $U_B \rightleftharpoons I_{alc}$ and $I_{alc} \rightleftharpoons U$ transitions at pH 13 (Figures 1 and 2).

in the effective number of water molecules that interact with any two states of the $U_B \rightleftharpoons I_{alc} \rightleftharpoons U$ equilibria. Third, because an alcohol can interact with both water and protein at the alkaline pH used in this study, water is strongly excluded from the unfolded chain. By corollary, the native state is preferentially hydrated.

We also considered the alcohol-induced unfolding process at pH 7 as a reference. Under this condition, horse cyt *c* has 21 positive charges and 15 negative charges, resulting in +6 net charges compared to a charge of −17 at pH 13. The unfolding transitions for methanol, ethanol, and propanol are now apparently two-state reactions (Supporting Information). Interestingly, values of $\Delta\zeta_w$ (Table 1) show that for both methanol and ethanol, the effective numbers of water molecules that interact across the $I_{alc} \rightleftharpoons U$ equilibrium at pH 13 and the $N \rightleftharpoons U$ equilibrium at pH 7 are closely comparable. Similarly, $\Delta\zeta_w$ values for the $U_B \rightleftharpoons U$ equilibrium at pH 13 and the $N \rightleftharpoons U$ equilibrium at pH 7 for propanol-induced unfolding are similar. These observations appear to suggest that the extent of perturbation of the chemical potential of an alcohol by the protein is indifferent to pH. However, U_B and N states are structurally not quite similar: the former is alkali-denatured (pH 13), and the latter has a native structure (pH 7). Also, the U state under the two pH conditions need not be structurally similar. These differences may produce a comparable balance of the ratio of the molal concentrations of water and protein for the two terminal states of the unfolding equilibrium under the two pH conditions (eq 2). Unfortunately, available data do not allow further discussion of this issue.

Alcohol-Induced Folding−Unfolding Kinetics. Because alcohols are generally believed to unfold proteins by disrupting the tertiary structures more than acting on secondary structures, kinetics of the folding−unfolding reaction should provide information about contraction and expansion of the polypeptide. A series of stopped-flow experiments was conducted in which cyt *c* held at pH 13 was allowed to refold and unfold at various mole fractions of methanol and butanol. Both refolding and unfolding kinetics are described by a submillisecond burst phase followed by two observable phases of widely separated rate constants (Figure 3a,b). For the sake of

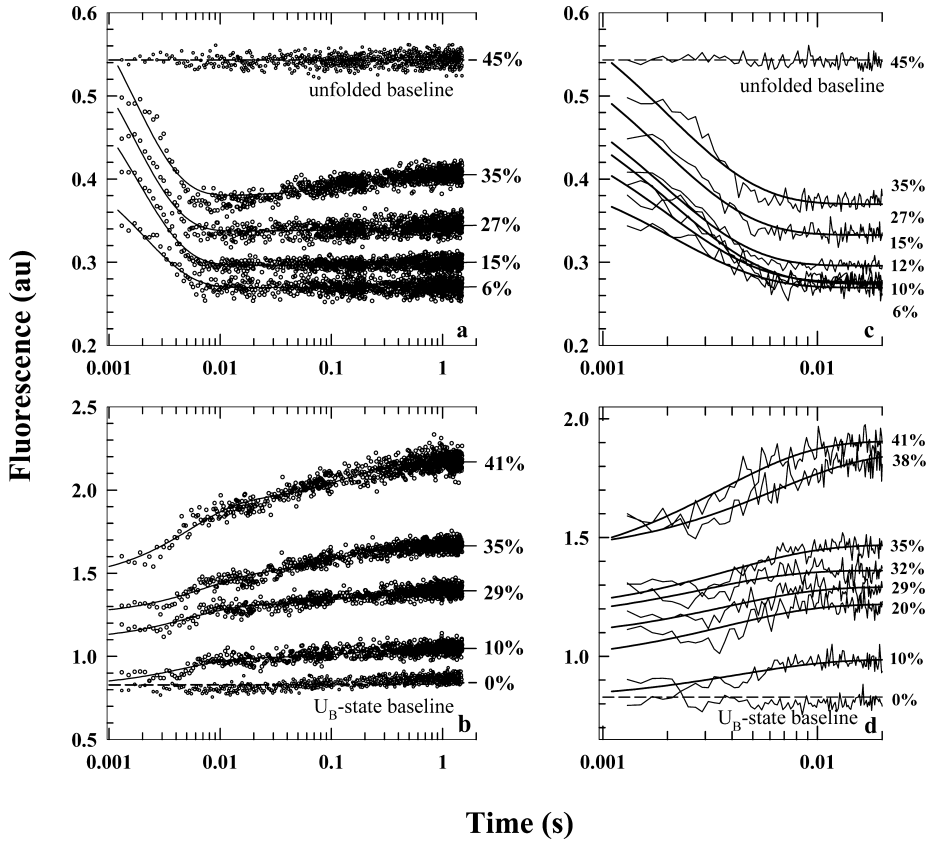

Figure 3. Stopped-flow kinetics for refolding and unfolding in the presence of butanol as indicated. (a) The refolding kinetics are described by a burst collapse followed by two observable exponentials. Of the two observed, the long-time exponential is negligible in both rate constant and amplitude. (b) Unfolding kinetics are characterized by a burst component followed by two exponentials in the observable window. (c) View of the first 20 ms of refolding traces (see panel a). (d) Expansion of the first 20 ms of unfolding traces.

dx.doi.org/10.1021/bi201716r | *Biochemistry* 2012, 51, 3273−3283

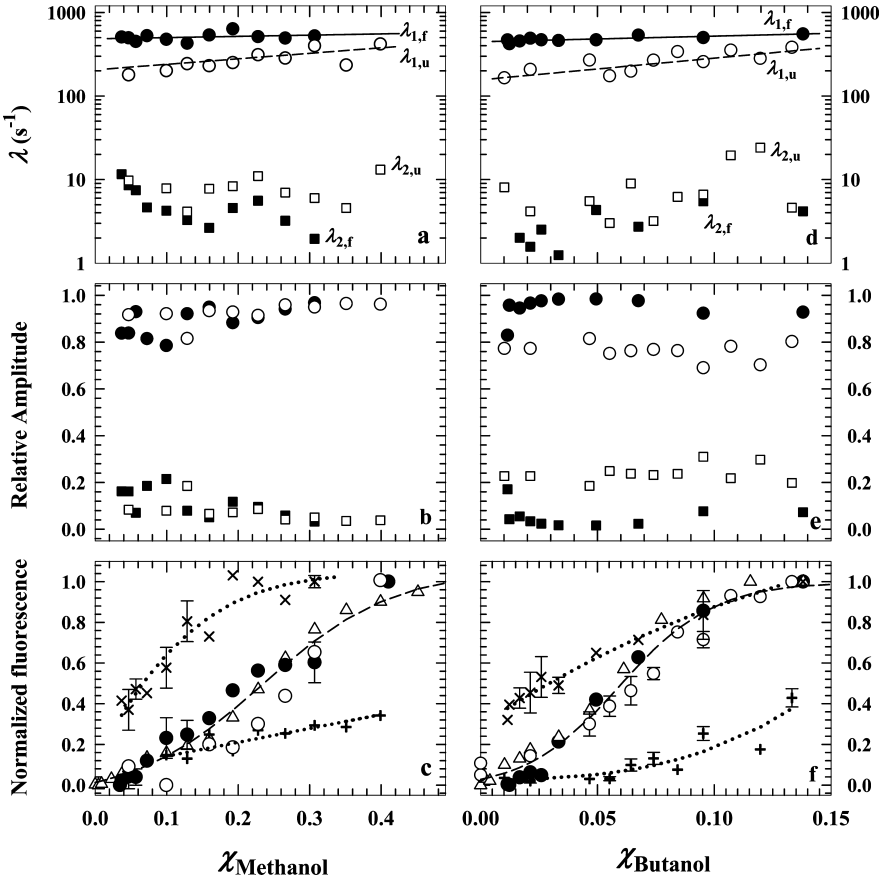

Figure 4. Variation of the observed two-exponential parameters with mole fractions of methanol (left) and butanol (right). (a and d) Two observable rate constants are obtained in both folding and unfolding reactions for all alcohols employed. Labels $\lambda_{1,f}$ (●) and $\lambda_{2,f}$ (■) stand for the fast phase and the slow phase of folding, respectively. Likewise, labels $\lambda_{1,u}$ (○) and $\lambda_{2,u}$ (□) denote the fast and slow unfolding phases, respectively. In all cases, $\lambda_{1,f} \gg \lambda_{2,f}$ and $\lambda_{1,u} \gg \lambda_{2,u}$. (b and e) The fast exponential of both folding and unfolding relaxation accounts for more than 80% of the total observable amplitude in all instances, allowing exclusion of the slow exponential from the description of a kinetic mechanism. (c and f) Fluorescence values read from refolding and unfolding kinetic traces at times t and ∞ (● and ○, respectively) are seen to reproduce the equilibrium data shown in Figure 1b (plotted here using △), suggesting that kinetics were recorded sufficiently long for the protein to relax to equilibrium. Although the alcohol dependence of the refolding burst amplitude (×) does not provide much information about the nature of the earliest temporal event, the nature of the observable phase (panels a and d and panels b and e) allows interpretation of the burst event as a hydrophobic collapse. On the other hand, as argued in the text, the unfolding burst phase (+) is likened to a nonspecific event. The lines through data points are drawn by inspection only. All experiments were conducted strictly at pH 13.

clarity, the fast observable phase and the missing kinetics are illustrated by the initial 20 ms of kinetics for several concentrations of butanol in panels c and d of Figure 3. The folding−unfolding kinetic traces obtained in the presence of methanol are very similar to these with regard to the number of phases and the sign of the fluorescence change.

The two rate constants for both folding ($\lambda_{1,f}$ and $\lambda_{2,f}$) and unfolding ($\lambda_{1,u}$ and $\lambda_{2,u}$) as a function of methanol and butanol concentration are shown in panels a and d of Figure 4, respectively. In all cases, the rate constants associated with the slow phase for folding and unfolding, $\lambda_{2,f}$ and $\lambda_{2,u}$, respectively, are tens fold smaller than those of the fast phase, $\lambda_{1,f}$ and $\lambda_{1,u}$, respectively. Further, the slow phase accounts for ∼15 ± 8% of the total observable amplitude (Figure 4b,e). These two observations suggest that the slow phase arises from a minor population of misfolded cyt *c* or perhaps due to a fraction of nonmonomeric protein that might exist under the extreme alkaline conditions that were used.[35] This phase will therefore be eliminated from further discussion, and the folding−unfolding reaction will be analyzed on the basis of the burst phase along with the observable fast phase ($\lambda_{1,f}$ and $\lambda_{1,u}$).

For both methanol and butanol, $\lambda_{1,f}$ responds little to the alcohol content in the refolding milieu (Figure 4a,d), suggesting that this phase hardly involves a change in the protein surface area. The surface burial event then must be completed in the submillisecond burst folding phase, but $\lambda_{1,u}$ discernibly increases by at least 2-fold in the range of alcohol concentrations used for unfolding (Figure 4a,d), implying considerable surface exposure. These considerations allow description of alcohol-induced folding and unfolding of alkaline cyt *c* by the minimal mechanism shown in Scheme 1:

Scheme 1

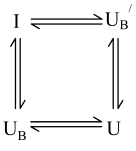

where U_B' is the burst folding intermediate that transforms to the denatured state U_B via a millisecond kinetic intermediate, I.

dx.doi.org/10.1021/bi201716r | *Biochemistry* 2012, 51, 3273−3283

The dependence of burst and observable amplitudes on alcohol concentration is quantified in panels c and f of Figure 4. The total change in fluorescence estimated from the steady state signal of the initial state and the signal at the completion of the kinetic course fairly coincides with the equilibrium unfolding data. The alcohol concentration dependence of the folding burst amplitudes should be ideally sigmoidal because the U → U_B' folding step is taken to involve the burial of virtually the entire protein surface required to be buried, but the nonavailability of kinetic folding data at alcohol concentrations lower than those shown as well as the error involved in the quantification of the burst amplitude precludes much discussion of the nature of the transition. As for unfolding, because of the lack of evidence for a specifically expanded ultrafast intermediate, the burst amplitude is considered simply an extension of the baseline.

The Equilibrium and Kinetic Unfolding Intermediates Are Configurationally Different. It is of interest to know if the intermediate detected in equilibrium experiments corresponds to the temporal burst intermediate inferred from kinetic results. Because the degree of expansion of the polypeptide directly relates to the extent of unfolding of the highly charged U_B state, we determined the mean effective hydrodynamic radius of the protein (R_h) at several concentrations of methanol by using pulsed field gradient NMR. The R_h value of 21.1 ± 1 Å in the absence of alcohol, fairly consistent with an earlier report,[35] increases to 36.5 ± 1.8 Å when the protein is placed in 60% methanol or a χ_{MeOH} of 0.4 (Figure 5). A comparison of R_h values obtained from this study with typical literature values for cyt *c* under different solvent conditions confirms that the extent of chain expansion induced by an alcohol is unusually large, suggesting that the alcohol-induced unfolded state cannot be compared with the ones produced by chaotropes, and hence, the mode of action of alcohol is distinct. Further, $R_h \sim 32$ Å at a χ_{MeOH} of ~0.1 where the equilibrium intermediate I_{alc} in the $U_B \rightleftharpoons I_{alc} \rightleftharpoons U$ mechanism populates (Figure 5). The data indicate that I_{alc} is roughly 30% less expanded than the fully unfolded protein at a χ_{MeOH} of 0.4, implying that the intermediate is closer to the unfolded state in terms of polypeptide expansion. This picture of a largely expanded chain in the equilibrium intermediate is inconsistent with a highly compact polypeptide in the burst kinetic intermediate. In fact, the latter can be inferred to be as compact as the native state because the intermediate I in the $I \rightleftharpoons U_B$ step of the proposed kinetic mechanism involves little surface burial (Figure 4a). These results suggest that the equilibrium and kinetic intermediates are different.

The hydrodynamic data can also be used to approximate an effective binding constant, K_B, for binding of methanol to the protein by a formalism similar to that used earlier by Makhatadze and Privalov to analyze binding isotherms of protein in urea and GdnHCl.[44] If many methanol molecules are assumed to bind to independent and identical apolar sites on the protein, then the dependence of R_h on the activity of methanol (a_{CH_3OH}) is

$$R_h = R_h^0\left(1 + r^{a\rightarrow 1}\frac{K_B a}{1 + K_B a}\right) \quad (3)$$

where R_h^0 is the hydrodynamic radius in water at pH 13 and $r^{a\rightarrow 1}$ is the relative change in the hydrodynamic radius as a_{CH_3OH} approaches unity. By applying this highly simplified binding model to the data (Figure 5b), one obtains a K_B of 4 ± 0.3

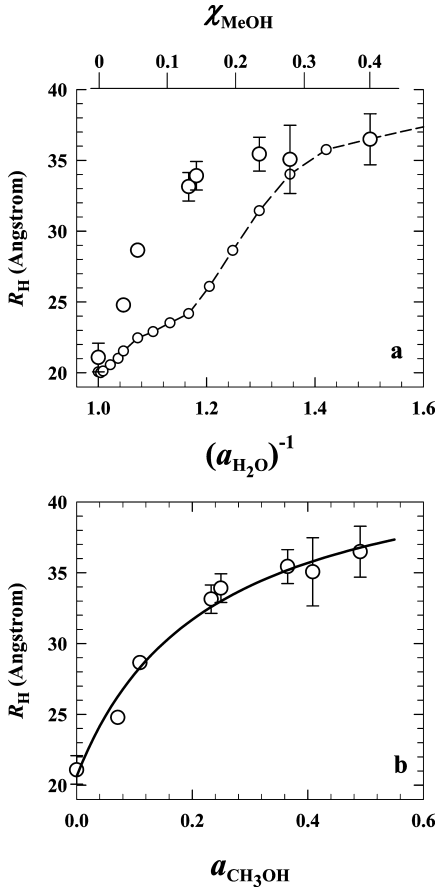

Figure 5. Variation of the hydrodynamic radius, R_h, of cyt *c* with increments of methanol at pH 13. (a) The expansion of the protein chain as measured by R_h (○) is shown along with the three-state equilibrium transition, $U_B \rightleftharpoons I_{alc} \rightleftharpoons U$ (small circles and dotted line) reproduced from Figure 1c. (b) The functional dependence of R_h on methanol activity (eq 2) is mapped by the solid line. The fit yields an effective binding constant (K_B = 4 ± 0.3) for binding of methanol to the hydrophobic sites of the protein.

at 22 °C that compares with the value of 0.013 for binding of CH_3OH to ribonuclease at 62 °C calculated from the theory of hydrophobic bond formation of Nemethy and Scheraga.[4,8] The binding energy for the interaction of CH_3OH with cyt *c* under our conditions ($-RT$ ln $K_B \sim 0.8$ kcal/mol) is in good agreement with literature values for the interaction of LUSH protein with alcohols at pH 4.[39,45] However, both hydrophobic interactions and hydrogen bonding contribute to the binding energy, and the data here cannot reveal the relative contributions of the two.

Structural Mobility in the Equilibrium Intermediate Is Relatively Restrained. Having observed a large increase in the hydrodynamic radius of the U_B state in the presence of alcohol at pH 13, we were interested to know the response of side chain motions under these conditions. The one-dimensional NMR spectrum of the initial state in the absence of alcohol is characterized by broad and poorly dispersed lines in both aliphatic and aromatic regions (Figure 6), indicating a general motional averaging of chemical shifts. This is to be expected because the U_B state by definition is the alkali-denatured state with a higher density of negative charges because of the exhaustive deprotonation of the side chains. The NMR lines are relatively sharp in the 10−20% range of methanol where the equilibrium intermediate populates, seen

dx.doi.org/10.1021/bi201716r | *Biochemistry* 2012, 51, 3273−3283

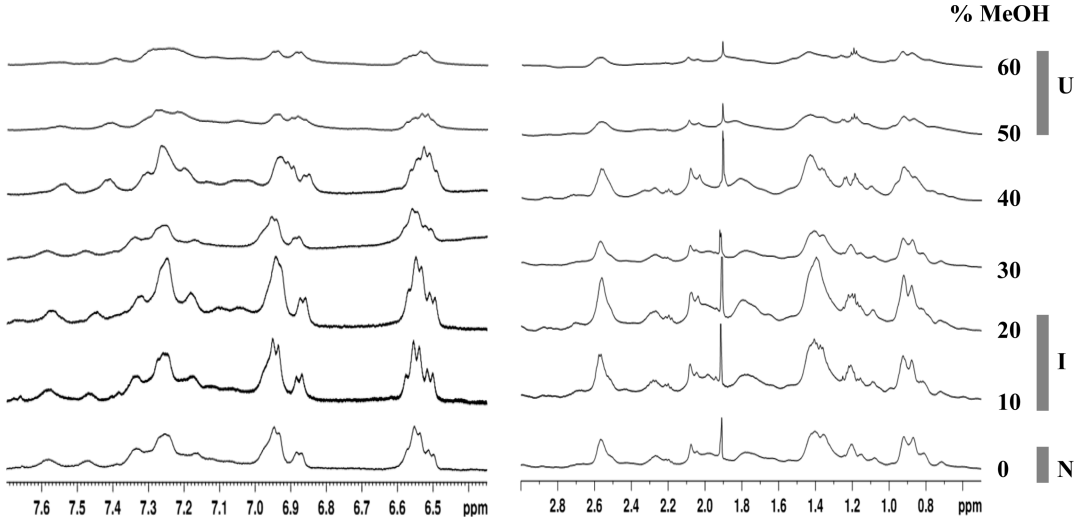

Figure 6. Resonances of the U_B state (pH 13) in the aliphatic and aromatic regions at different concentrations of CD_3OD. Initial increments of the alcohol up to ~20%, where the equilibrium intermediate populates, produce relatively sharp resonances. Further increments of alcohol cause line broadening and more deteriorated dispersion.

more clearly for the aromatic side chain resonances (Figure 6), implying a general constraint on the rotational motion and environmental averaging in the intermediate state. As the $I_{alc} \rightleftharpoons U$ transition is approached by the increase in the methanol concentration, the resonances increasingly broaden with deteriorating dispersion. At 60% methanol (U state) where the unfolded chain is enormously expanded (R_h = 36.5 Å), the resonances are smeared and the side chains exhibit extreme motional averaging.

NOE Constraints in the Intermediate. Because the equilibrium intermediate is characterized by a large hydrodynamic radius (R_h ~ 32 Å) and thus appeared closer to the unfolded state (Figure 5), it was important to check for the presence of tertiary interactions. The NOESY spectrum of the U_B state is virtually bare except for a prominent cluster of positive NOE cross-peaks likely to arise from dipolar interactions between Tyr ring protons and β/γ side chain protons of unknown residues (Figure 6). These interactions (<5−6 Å) are conducted with alcohol increments up to ~30% MeOH and vanish thereafter, suggesting the presence of some tertiary contacts in the intermediate state even though the polypeptide chain may be largely expanded. The persistence of detectable positive NOE peaks also suggests that the global correlation time (τ_c) of the folding intermediate is greater than ~2 ns, because the NOE should vanish when $\omega_o\tau_c \approx 1$, where ω_o is the Larmor frequency, 500 MHz.

DISCUSSION

Effects of alkyl alcohols on the structure and reactivity of cyt *c* under neutral-pH conditions have been studied for many years. Some of the earliest studies reported on the influence of alcohols on the disruption of structure in the vicinity of the heme and changes in the rate of autoxidation of ferrocytochrome *c* arising thereof.[46,47] Equilibrium aspects of the conformation and unfolding of the cyt *c* chain in the presence of alcohols are also being addressed since then.[8] The binding of alcohol to cyt *c*,[37] the occurrence of structural intermediates in methanol-induced unfolding at low pH,[23] and partial unfolding in the presence of benzyl alcohol[48] have also been reported. The major thrust of this work is to learn about the thermodynamic and kinetic aspects of alcohol-induced unfolding of a highly charged protein. According to the nature of the objective, the folding−unfolding reaction of cyt *c* was studied at pH 13 in the absence of ionic strength. The protein under such conditions is charge-imbalanced with a net negative charge of −17.

Electrostatic Response of a Dense Negatively Charged Protein Placed in Alcohol. Charged polar side chains of folded proteins in aqueous solvent are generally located on the outer surface, where they are favorably solvated.[49] However, the stability of internally charge-rich proteins rests on the polarity, concentration, and location of charges in the perspective of atomic structural details in a rather complex manner. In the macroscopic approach based on Tanford−Kirkwood treatment,[50] burial of charges is energetically expensive simply because the protein interior is taken as a general medium with a low dielectric constant (ε) where the charge storage capacity is very low. Numerous proteins of reputed stability harboring internal charges are, however, known where the cost of charge burial is alleviated because of the location of the charges in polar surroundings produced by several factors,[51] including polar side chains, internal water molecules, and fluctuating protein dipoles. Because of internal charge accommodating provisions, buried charges usually do not pose a serious threat to protein stability. It follows that the disposition of unscreened surface charges in response to the decreasing activity of water from unity, as would happen with an increasing level of alcohol in the water/alcohol mixture, is a key factor leading to structural unfolding. For the experimental condition of pH 13, the net charge on the nativelike U_B state used here is −17, which makes the protein surface highly negatively charged. The repulsive Coulombic forces between surface charges grow stronger as the dielectric constant of the bulk solvent is decreased with an increase in the mole fraction of alcohols. The increasing force of anion repulsion then drives the protein to expand. The effectiveness of the alcohol increases as its dielectric constant decreases with an increasing hydrocarbon content. The significance of this apparently simple explanation would vary according to the charge polarity, ionic strength of the medium, and solvent dielectric. In a neutral-pH aqueous solvent, the electrostatic repulsion of surface charges may not be important,[8,9,52,53] but under the highly alkaline

dx.doi.org/10.1021/bi201716r | *Biochemistry* 2012, 51, 3273−3283

low-ionic strength conditions employed here, the increasing repulsive force in the low-dielectric solvent assumes high significance. In fact, electrostatic destabilization produced at low pH was found to decrease the midpoint of ethanol-induced denaturation of chymotrypsinogen.[2] This factor was not studied in detail previously, perhaps because of the discouraging suggestion that electrostatic effects may be safely neglected.[8]

The electrostatic interpretation suggests that it is the dielectric constant of the medium alone that generates the driving force for unfolding; the type or identity of the alcohol is irrelevant (Figure 1a) even though the mole fraction scale of the alcohol required to obtain a given range of ε value shrinks as the volume of the alkyl side chain in the alcohol increases (Figure 1b). Such normalization of unfolding data with respect to dielectric constants of alcohols, reported previously by Wilkinson and Mayer,[13] implies that it is the molar volume rather than the mole fraction or volume fraction of alcohol that is important. By corollary, the higher the hydrophobicity, the more effective the alcohol (Figure 1b).

Protein−Alcohol Interactions under Alkaline Conditions. The binding model involving weak protein−denaturant interactions has been put into a complete general form.[5,54,55] Although the nature of alcohol−protein interactions has not been fully understood, accumulated evidence strongly indicates that the interactions are predominantly hydrophobic in nature,[9,10,22,56−59] affecting both local and nonlocal structures.[14,17,21,60,61] A particularly interesting situation arises under highly alkaline conditions where the solution pH approaches pK_a values of solvent components and protein main chain amides; estimated values of pK_a are 15.7 for water, 15.2−17 for primary alcohols, and 18 for the peptide NH group.[62,63] As shown below, several modes of peptide−water and peptide−alcohol hydrogen bonding are possible. Clearly, existing

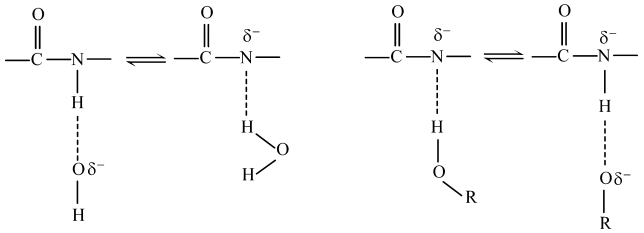

secondary structural elements will be destabilized. This action of alcohol, valid under strongly alkaline conditions, is the opposite of the well-known helix-stabilizing effect observed under neutral-pH conditions.[14,16,64−66]

The peptide−water and peptide−alcohol hydrogen bonding interactions do not negate the occurrence of alcohol−protein hydrophobic interactions. The hydrocarbon group of alcohols should bind to apolar side chains, because they form the bulk of the hydrophobic surface in the protein interior. The association constants, K_B, for the binding of different alcohols to an average hydrophobic cluster in the protein increases with an increasing hydrocarbon content of alcohols;[4,8] the larger the K_B value, the more effective the alcohol is toward protein unfolding observed earlier and in this study (Figure 1b,c). Thus, although alcohols act on proteins in alkaline medium by both H-bonding and hydrophobic interactions, the observed alkyl chain-based effectiveness (Figure 1b) still indicates the latter's dominance in protein unfolding.

Hydrophobic Collapse Dominates Folding Kinetics. Charge repulsion in the alcohol-unfolded alkaline cyt *c* persists, much stronger than in the aqueous solution under identical solution conditions. When the alcohol-unfolded protein is allowed to refold by dilution of the solution into water at the same alkaline pH of 13, two strongly opposing forces come into operation: the hydrophobic attractive force that drives the chain to collapse and the electrostatic repulsive force resisting chain contraction. Looking at the kinetic results, one finds that the stopped-flow burst folding phase accounts for burial of virtually the entire surface that is buried in the U_B state, and the observable millisecond phase corresponds to relatively slower chain compaction with little surface burial (Figure 4 and Scheme 1). This result strongly argues for a microsecond hydrophobic collapse driven by dissociation of the bound hydrocarbon part of alcohols from the hydrophobic surfaces of the unfolded protein chain. Clearly, the hydrophobic force prevails over the electrostatic drag. The collapse constrains the chain topology and the location of the charged amino acids and weakens the electrostatic destabilization.

Preferential Exclusion of Water and the Equilibrium Unfolding Intermediate, I_{alc}. Because proteins are preferentially hydrated when placed in stabilizing cosolvents like glycerol and polyols,[40,67] alcohol destabilization should produce preferential exclusion of water molecules from the protein vicinity as is seen in Figure 2. The finding that the effective number of departing water molecules increases with an increasing hydrocarbon content, $\Delta\zeta_w$ (eq 1), is an indicator of the unfolding effectiveness of cosolvents. This is a general result. In the context of alkaline cyt *c*, it is interesting that

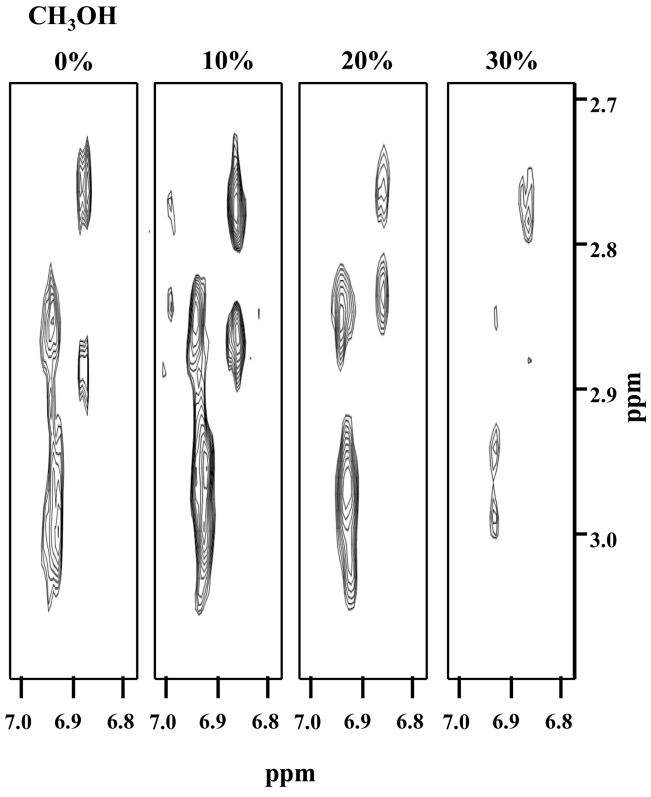

Figure 7. Cluster of NOE cross-peaks arising from dipolar interaction between aromatic ring protons and most likely $C_\beta H$ or $C_\varepsilon H$ protons. A few additional cross-peaks appear at the initial increments of methanol, shown by the 10% methanol spectrum. The interactions gradually weaken as the alcohol concentration is increased to 30%.

dx.doi.org/10.1021/bi201716r | *Biochemistry* 2012, 51, 3273−3283

roughly 85% of the total number of excluded water come from the $U_B \rightleftharpoons I_{alc}$ segment of the $U_B \rightleftharpoons I_{alc} \rightleftharpoons U$ equilibrium (Table 1), implying that the extent of preferential exclusion of water from I_{alc} is only slightly less than that from U_B. The equilibrium intermediate is thus substantially unfolded, lacking internal cavity waters that have already departed to the solvent.

The I_{alc} Intermediate Is Unlikely To Be a Dry Molten Globule (DMG). A relatively lesser known class of intermediates considered in literature is the DMG defined qualitatively as an expanded state of the native fold lacking both internal hydration and close packing of side chains but retaining the nativelike backbone structure.[68] The I_{alc} intermediate of our study is devoid of intrinsic water molecules and is expanded to the extent of ~40% relative to the native fold (Figure 5), appearing to suggest its inclusion in the DMG class. However, the finding of side chain NOEs in the I_{alc} intermediate, albeit fewer in number, indicates the presence of tertiary contacts (Figure 7) and hence an apparent disqualification for DMG. A general constraint on side chain rotations and environmental averaging as revealed by sharp resonances in the 10−20% range of methanol (Figure 6) further argues against a comparable picture of I_{alc} and DMG, because the latter is proposed to have higher conformational entropy.[68] Until additional results on the nature of the I_{alc} state are available, it may simply be taken as a general structural intermediate of alkaline cyt *c* without committing it to the MG or DMG.

■ ASSOCIATED CONTENT

Supporting Information

Alcohol-induced equilibrium unfolding data and plots for extraction of preferential water exclusion at pH 7. This material is available free of charge via the Internet at http://pubs.acs.org.

■ AUTHOR INFORMATION

Corresponding Author

*School of Chemistry, University of Hyderabad, Hyderabad 500 046, India. E-mail: akbsc@uohyd.ernet.in. Phone: 91-40-2313-4810.

Author Contributions

A.K.B. generated ideas and designed the research. P.S., U.M.Y., and A.K.B. performed the research. P.S., U.M.Y., and A.K.B. analyzed the data. A.K.B. wrote the paper.

Funding

This research was supported by grants from Departments of Biotechnology (BRB/15/227/2001 and BRB/10/622/2008) and Science and Technology (4/1/2003-SF) to A.K.B.

Notes

The authors declare no competing financial interest.

■ ABBREVIATIONS

cyt *c*, cytochrome *c*; U_B, cytochrome *c* at pH 13 or the compact alkali-denatured state; I_{alc}, equilibrium intermediate in the presence of alcohol; U_B', burst intermediate; I, late kinetic intermediate; GdnHCl, guanidinium hydrochloride; ε, dielectric constant; R_h, hydrodynamic radius; $\chi_{alcohol}$, mole fraction of alcohol; a_{H_2O}, activity of water; a_{CH_3OH}, activity of methanol; MG, molten globule; DMG, dry molten globule.

■ REFERENCES

(1) Schrier, E. E., and Scheraga, H. A. (1962) The effect of aqueous alcohol solutions on the thermal transition of ribonuclease. *Biochim. Biophys. Acta 64*, 406−408.

(2) Brandts, J. F. (1964) The thermodynamics of protein denaturation. I. The denaturation of chymotrypsinogen. *J. Am. Chem. Soc. 86*, 4291−4301.

(3) Brandts, J. F., and Hunt, L. (1967) The thermodynamics of protein denaturation. 3. The denaturation of ribonuclease in water and in aqueous urea and aqueous ethanol mixtures. *J. Am. Chem. Soc. 89*, 4826−4838.

(4) Schrier, E. E., Ingwall, R. T., and Scheraga, H. A. (1965) The effect of aqueous alcohol solutions on the thermal transition of ribonuclease. *J. Phys. Chem. 69*, 298−303.

(5) Peller, L. (1959) On a model for the helix-random coil transition in polypeptides. II. The influence of solvent composition and charge interactions on the transition. *J. Phys. Chem. 63*, 1199−1206.

(6) Flory, P. J., and Miller, W. G. (1966) A general treatment of helix-coil equilibria in macromolecular systems. *J. Mol. Biol. 15*, 284−297.

(7) Nemethy, G., and Scheraga, H. A. (1962) The structure of water and hydrophobic bonding in proteins. III. The thermodynamic properties of hydrophobic bonds in proteins. *J. Phys. Chem. 66*, 1773−1789.

(8) Herskovits, T. T., Gadegbeku, B., and Jaillet, H. (1970) On the structural stability and solvent denaturation of proteins. I. Denaturation by the alcohols and glycols. *J. Biol. Chem. 245*, 2588−2598.

(9) Tanford, C. (1968) Protein denaturation. *Adv. Protein Chem. 23*, 121−282.

(10) Timasheff, S. N. (1970) Protein-solvent interactions and protein conformation. *Acc. Chem. Res. 3*, 62−68.

(11) Timasheff, S. N., and Inoue, H. (1968) Preferential binding of solvent components to proteins in mixed water-organic solvent systems. *Biochemistry 7*, 2501−2513.

(12) Franks, F., and Eagland, D. (1975) The role of solvent interactions in protein conformation. *CRC Crit. Rev. Biochem. 3*, 165−219.

(13) Wilkinson, K. D., and Mayer, A. N. (1986) Alcohol-induced conformational changes of ubiquitin. *Arch. Biochem. Biophys. 250*, 390−399.

(14) Nelson, J. W., and Kallenbach, N. R. (1986) Stabilization of the ribonuclease S-peptide α-helix by trifluoroethanol. *Proteins: Struct., Funct., Genet. 1*, 211−217.

(15) Lehrman, S. R., Tuls, J. L., and Lund, M. (1990) Peptide α-helicity in aqueous TFE: Correlations with predicted α-helicity and the secondary structure of the corresponding regions of bovine growth hormone. *Biochemistry 29*, 5590−5596.

(16) Segawa, S.-I., Fukono, T., Fujiwara, K., and Noda, Y. (1991) Local structures in unfolded lysozyme and correlation with secondary structures in the native conformation: Helix-forming and -breaking propensity of peptide segments. *Biopolymers 31*, 497−509.

(17) Harding, M. M., Williams, D. H., and Woolfson, D. N. (1991) Characterization of a partially denatured state of a protein by two-dimensional NMR: Reduction of the hydrophobic interactions in ubiquitin. *Biochemistry 30*, 3120−3128.

(18) Sönnichsen, F. D., van Eyk, J. E., Hodges, R. S., and Sykes, B. D. (1992) Effect of TFE on protein secondary structure: An NMR and CD study using a synthetic actin peptide. *Biochemistry 31*, 8790−8798.

(19) Dyson, H. J., Sayre, J. R., Merutka, G., Shin, H.-C., Lerner, R. A., and Wright, P. W. (1992) Folding of peptide fragments comprising the complete sequence of proteins: Models for initiation of protein folding II. Plastocyanin. *J. Mol. Biol. 226*, 818−835.

(20) Dufour, E., Bertrand-Harb, C., and Haertlé, T. (1993) Reversible effects of medium dielectric constant on structural transformation of β-lactoglobulin and its retinol binding. *Biopolymers 33*, 589−598.

(21) Buck, M., Radford, S. E., and Dobson, C. M. (1993) A partially folded state of hen egg white lysozyme in trifluoroethanol: Structural characterization and implications for protein folding. *Biochemistry 32*, 669−678.

(22) Thomas, P. D., and Dill, K. A. (1993) Local and non-local interactions in globular proteins and mechanisms of alcohol denaturation. *Protein Sci. 2*, 2050−2065.

(23) Kamatari, Y. O., Konno, T., Kataoka, M., and Akasaka, K. (1996) The methanol-induced globular and expanded denatured states of cytochrome *c*: A study by CD, fluorescence, NMR and small-angle X-ray scattering. *J. Mol. Biol. 259*, 512−523.
(24) Kentsis, A., and Sosnick, T. R. (1998) Trifluoroethanol promotes helix formation by destabilizing backbone exposure: Desolvation rather than native hydrogen bonding defines the kinetic pathway of dimeric coiled coil folding. *Biochemistry 37*, 14613−14622.
(25) Hirota, N., Mizuno, K., and Goto, Y. (1998) Group additive contributions to the alcohol-induced α-helix formation of melittin: Implication for the mechanism of the alcohol effects on proteins. *J. Mol. Biol. 275*, 365−378.
(26) Buck, M. (1998) Trifluoroethanol and colleagues: Cosolvents come of age. Recent studies with peptides and proteins. *Q. Rev. Biophys. 31*, 287−355.
(27) Kamatari, Y. O., Konno, T., Kataoka, M., and Akasaka, K. (1998) The methanol-induced transition and the expanded helical conformation of hen lysozyme. *Protein Sci. 7*, 681−688.
(28) Shimizu, S., and Shimizu, K. (1999) Alcohol denaturation: Thermodynamic theory of peptide unit salvation. *J. Am. Chem. Soc. 121*, 2387−2394.
(29) Sasahara, K., and Nitta, K. (2006) Effect of ethanol on folding of hen egg-white lysozyme under acidic condition. *Proteins: Struct., Funct., Bioinf. 63*, 127−135.
(30) Miyawaki, O., and Tatsuno, M. (2011) Thermodynamic analysis of alcohol on thermal stability of proteins. *J. Biosci. Bioeng. 11*, 198−203.
(31) Martin, S. R., Esposito, V., De Los Rios, P., Pastore, A., and Temussi, P. A. (2008) Cold denaturation of yeast frataxin offers the clue to understand the effect of alcohols on protein stability. *J. Am. Chem. Soc. 130*, 9963−9970.
(32) Kumar, R., Prabhu, N. P., and Bhuyan, A. K. (2005) Ultrafast events in the folding of ferrocytochrome *c*. *Biochemistry 44*, 9359−9367.
(33) Kumar, R., Prabhu, N. P., Rao, D. K., and Bhuyan, A. K. (2006) The alkali molten globule state of horse ferricytochrome c: Observation of cold denaturation. *J. Mol. Biol. 364*, 483−495.
(34) Bhuyan, A. K. (2009) On the mechanism of SDS-induced protein denaturation. *Biopolymers 93*, 186−199.
(35) Bhuyan, A. K. (2010) Off-pathway status for the alkali molten globule of horse ferricytochrome *c*. *Biochemistry 49*, 7764−7773.
(36) Bhuyan, A. K. (2010) The off-pathway status of the alkali molten globule is unrelated to heme misligation and trans-pH effects: Experiments with ferrocytochrome *c*. *Biochemistry 49*, 7774−7782.
(37) Muhoberac, B. B., and Brill, A. S. (1980) Association of alcohols with heme proteins: Optical analysis and thermodynamic models. *Biochemistry 19*, 5157−5167.
(38) Dwyer, D. S., and Bradley, R. J. (2000) Chemical properties of alcohols and their protein binding sites. *Cell. Mol. Life Sci. 57*, 265−275.
(39) Thode, A. B., Kruse, A. W., Nix, J. C., and Jones, D. N. M. (2008) The role of multiple hydrogen-bonding groups in specific alcohol binding sites in proteins: Insights from structural studies of LUSH. *J. Mol. Biol. 376*, 1360−1376.
(40) Timasheff, S. N. (2002) Protein-solvent preferential interactions, protein hydration, and the modulation of biochemical reactions by solvent components. *Proc. Natl. Acad. Sci. U.S.A. 99*, 9721−9726.
(41) Wyman, J. Jr. (1964) Linked functions and reciprocal effects in hemoglobin: A second look. *Adv. Protein Chem. 19*, 223−286.
(42) Tanford, C. (1969) Extension of the theory of linked functions to incorporate the effects of protein hydration. *J. Mol. Biol. 39*, 539−544.
(43) Gekko, K., and Timasheff, S. N. (1981) Thermodynamic and kinetic examination of protein stabilization by glycerol. *Biochemistry 20*, 4677−4686.
(44) Makhatadze, G. I., and Privalov, P. L. (1992) Protein interactions with urea and guanidinium chloride: A calorimetric study. *J. Mol. Biol. 226*, 491−505.
(45) Shahidullah, M., Harris, T., Germann, M. W., and Covarrubias, M. (2003) Molecular features of an alcohol binding site in a neuronal potassium channel. *Biochemistry 42*, 11243−11252.
(46) Kaminsky, L. S., and Davison, A. J. (1969) Effects of organic solvents on the spectrum of cytochrome *c*. *Biochemistry 8*, 4631−4637.
(47) Kaminsky, L. S., Wright, R. L., and Davison, A. J. (1971) Effect of alcohols on the rate of autoxidation of ferrocytochrome *c*. *Biochemistry 10*, 458−462.
(48) Singh, S. M., Cabello-Villegas, J., Hutchings, R. L., and Mallela, K. M. G. (2010) Role of partial protein unfolding in alcohol-induced protein aggregation. *Proteins 78*, 2625−2637.
(49) Perutz, M. F. (1978) Electrostatic effects in proteins. *Science 201*, 1187−1191.
(50) Tanford, C., and Kirkwood, J. G. (1957) Theory of protein titration curves. I. General equations for impenetrable spheres. *J. Am. Chem. Soc. 79*, 5333−5339.
(51) Warshel, A., Russell, S. T., and Churg, A. K. (1984) Macroscopic models for studies of electrostatic interactions in proteins: Limitations and applicability. *Proc. Natl. Acad. Sci. U.S.A. 81*, 4785−4789.
(52) Bodkinand, M. J., and Goodfellow, J. M. (1996) Hydrophobic salvation in aqueous trifluoroethanol solution. *Biopolymers 39*, 43−50.
(53) Del Vecchio, P., Graziano, G., Granata, V., Barone, G., Mandrich, L., Rossi, M., and Manco, G. (2003) Effect of trifluoroethanol on the conformational stability of a hyperthermophilic esterase: A CD study. *Biophys. Chem. 104*, 407−415.
(54) Schellman, J. A. (1975) Macromolecular binding. *Biopolymers 14*, 999−1018.
(55) Schellman, J. A. (2002) Fifty years of solvent denaturation. *Biophys. Chem. 96*, 91−101.
(56) Von Hippel, P. H., and Wong, K. Y. (1965) On the conformational stability of globular proteins. The effects of various electrolytes and nonelectrolytes on the thermal ribonuclease transition. *J. Biol. Chem. 240*, 3909−3923.
(57) Gerlsma, S. Y. (1968) Reversible denaturation of ribonuclease in aqueous solutions as influenced by polyhydric alcohols and some other additives. *J. Biol. Chem. 243*, 957−961.
(58) Parodi, R. M., Bianchi, E., and Ciferri, A. (1973) Thermodynamics of unfolding of lysozyme in aqueous alcohol solutions. *J. Biol. Chem. 248*, 4047−4051.
(59) Arakawa, T., and Goddette, D. (1985) The mechanism of helical transition of proteins by organic solvents. *Arch. Biochem. Biophys. 240*, 21−32.
(60) Fan, P., Bracken, C., and Baum, J. (1993) Structural characterization of monellin in the alcohol-denatured state by NMR: Evidence for β-sheet to α-helix conversion. *Biochemistry 32*, 1573−1582.
(61) Alexendrescu, A. T., Ng, Y.-L., and Dobson, C. M. (1994) Chracterization of a TFE-induced partially folded state of α-lactalbumin. *J. Mol. Biol. 235*, 587−599.
(62) Molday, R. S., and Kallen, R. G. (1972) Substituent effects on amide hydrogen exchange rates in aqueous solutions. *J. Am. Chem. Soc. 94*, 6739−6745.
(63) Eriksson, M. A. L., Härd, T., and Nilsson, L. (1995) On the pH dependence of amide proton exchange rates in proteins. *Biophys. J. 69*, 329−339.
(64) Nelson, J. W., and Kallenbach, N. R. (1989) Persistence of the α-helix stop signal in the S-peptide in trifluoroethanol. *Biochemistry 28*, 5256−5261.
(65) Kippen, A. D., Sancho, J., and Fersht, A. R. (1994) Folding of barnase in parts. *Biochemistry 33*, 3778−3786.
(66) Siraki, K., Nishikawa, K., and Goto, Y. (1995) Trifluoroethanol-induced stabilization of the α-helical structure of β-lactoglobulin: Implication for non-hierarchical protein folding. *J. Mol. Biol. 245*, 180−194.

(67) Gekko, K., and Timasheff, S. N. (1981) Mechanism of protein stabilization by glycerol: Preferential hydration in glycerol-water mixtures. *Biochemistry 20*, 4667−4676.
(68) Baldwin, R. L., Frieden, C., and Rose, G. D. (2010) Dry molten globule intermediates and the mechanism of protein folding. *Proteins 78*, 2725−2737.